Construction and Floquet–Bloch analysis of analytically solvable Hill equations with smooth potentials

Ibrahim, A.; Sprung, D.W.L.; Morozov, G.V.

Published in:
Journal of the Optical Society of America B

DOI:
10.1364/JOSAB.35.001223

Published: 02/05/2018

Document Version
Peer reviewed version

Ibrahim, A., Sprung, D. W. L., & Morozov, G. V. (2018). Construction and Floquet–Bloch analysis of analytically solvable Hill equations with smooth potentials. Journal of the Optical Society of America B, 35(6), 1223-1232. https://doi.org/10.1364/JOSAB.35.001223

Construction and Floquet-Bloch analysis of analytically solvable Hill equations with smooth potentials

A. IBRAHIM[1], D. W. L. SPRUNG[1], AND G. V. MOROZOV[2,*]

[1] Department of Physics and Astronomy, McMaster University, Hamilton L8S 4M1, Ontario, Canada
[2] Scottish Universities Physics Alliance (SUPA), Institute of Thin Films, Sensors and Imaging, University of the West of Scotland, Paisley PA1 2BE, UK
[*] Corresponding author: gregory.morozov@uws.ac.uk

Compiled April 4, 2018

We construct analytically solvable Hill equations with smooth potentials and smooth solutions using a method of Wu and Shih. We then use Floquet-Bloch theory to analyze the band structure and find the Floquet-Bloch fundamental system of solutions of the resulting differential equation. Three examples of constructed potentials and their corresponding solutions are worked out.

OCIS codes: (050.5298) Photonic crystals; (260.2110) Electromagnetic optics;(000.3860) Mathematical methods in physics.

http://dx.doi.org/10.1364/ao.XX.XXXXXX

1. INTRODUCTION

Many problems in physics and engineering require solution of a second-order differential equation taking the form

$$\frac{\mathrm{d}^2\Psi}{\mathrm{d}z^2} + Q(z)\Psi(z) = 0. \tag{1}$$

If a periodic system is considered, then $Q(z+d) = Q(z)$, where d is the period. We then call Eq. (1) a Hill equation. In quantum mechanics, for example, the periodic Schrödinger Equation has the form $Q(z) = (2m/\hbar^2)[E - V(z)]$, where $V(z+d) = V(z)$ is a periodic potential [1]. We can also describe one-dimensional photonic crystals with a periodic refractive index $n(z+d) = n(z)$ using Eq. (1). In the case of normal incidence, we deal with Hill equations with $Q(z) = k_0^2 n^2(z)$, **where k_0 is the vacuum wavenumber of light propagating through the crystal,** to find the electric field inside the crystal [2]. Being able to construct analytically solvable Hill equations of continuous potentials could be a useful tool for modeling optical systems. For brevity, we will refer to $Q(z)$ as a potential throughout the remainder of this paper.

Hill equations are often analyzed using Floquet-Bloch theory because it provides a way of finding both their band structures and their solutions in terms of the Floquet-Bloch functions (also called the Floquet-Bloch fundamental system of solutions). Those solutions are convenient because one of their properties allows us to map them over all space when they are known on one period [3].

The **overall number** of analytically solvable Hill equations is small. Some examples are discontinuous periodic potentials, including piecewise constant potentials and sawtooth potentials [2, 4]. Several solvable Hill equations with continuous periodic potentials were found in the 1980's [5–8], but their solutions are not immediately smooth, which limits their use in physical problems. However, they can be modified to become smooth, while still satisfying their corresponding Hill equations [9, 10].

In this paper we generate three new analytically solvable Hill equations and their solutions using a method introduced by Wu and Shih [8]. We then use Floquet-Bloch theory to find the band structure of each potential and the forms of the Floquet-Bloch solutions in each region of the band structure. **All three newly obtained analytically solvable Hill equations have continuous periodic potentials $Q(z)$, thus, making the following analysis somewhat relevant to the studies of optical rugate filters, which are based on 1D photonic crystals with a sinusoidal refractive index profile [11].**

2. CONSTRUCTING HILL EQUATIONS AND SOLUTIONS

The details of derivation were presented by Wu and Shih [8]. To begin, we choose a relatively simple Hill equation with a periodic smooth potential $f(z)$ having period d

$$\frac{\mathrm{d}^2\Psi}{\mathrm{d}z^2} + f(z)\Psi(z) = 0. \tag{2}$$

If $\psi_0(z)$ is a periodic particular solution to Eq. (2), then $f(z)$ satisfies

$$f(z) = -\frac{1}{\psi_0}\frac{\mathrm{d}^2\psi_0}{\mathrm{d}z^2}. \tag{3}$$

We use $f(z)$ and $\psi_0(z)$ to construct a more complicated Hill equation whose potential takes the form

$$Q(z,a) = \frac{a}{[\psi_0(z)]^4} + f(z), \tag{4}$$

where a is an arbitrary real constant. The solutions to the Hill equation with this potential are

$$\psi_1(z) = A_1\psi_0(z)\cos[\Phi_1(z)], \tag{5}$$
$$\psi_2(z) = A_2\psi_0(z)\sin[\Phi_1(z)], \tag{6}$$

where the phase integrals $\Phi_1(z)$ and $\Phi_2(z)$ are

$$\Phi_{1,2}(z) = \sqrt{a}\int_0^z \frac{\mathrm{d}r}{[\psi_0(r)]^2} + C_{1,2}. \tag{7}$$

The constants A_1, A_2, C_1, and C_2 are chosen to satisfy the normalization conditions $\psi_1(0) = 1$, $\psi_1'(0) = 0$, $\psi_2(0) = 0$, and $\psi_2'(0) = 1$. $\Phi_1(z)$ and $\Phi_2(z)$ may have to be modified to make them continuous, as was done in [9, 10]. Finally, these normalized solutions are used to construct the Floquet-Bloch fundamental system for this Hill equation.

The initial particular solution $\psi_0(z)$ should be chosen bearing in mind that we would prefer to have Eqs. (4) and (7) continuous without modification. Motivated by this, we pick a particular solution in the form

$$\psi_0(z) = \frac{1}{\sqrt{g(z)}}, \tag{8}$$

where $g(z)$ is a smooth, nonvanishing, and integrable periodic function of period d. Following the procedure laid out by Wu and Shih, we derive Eqs. (4) and (7) in their respective forms

$$Q(z,a) = a[g(z)]^2 + \frac{1}{2}\frac{1}{g(z)}\frac{\mathrm{d}^2 g}{\mathrm{d}z^2} - \frac{3}{4}\frac{1}{[g(z)]^2}\left(\frac{\mathrm{d}g}{\mathrm{d}z}\right)^2, \tag{9}$$

and

$$\Phi_{1,2}(z) = \sqrt{a}\int_0^z g(r)\mathrm{d}r + C_{1,2}. \tag{10}$$

It should be noted that if a is very large or $g(z)$ varies sufficiently slowly with z, Eq. (9) and (10) arise in the WKB approximation, as remarked by Renne [12].

3. FLOQUET-BLOCH THEORY

The Hill differential equation gives rise to several fundamental systems of solutions, but the one of particular interest to us is the Floquet-Bloch system [3, 13, 14]. It always contains at least one (nontrivial) solution $F_1(z)$, called the Floquet-Bloch wave, with the property

$$F_1(z+d) = \rho_1 F_1(z), \tag{11}$$

where ρ_1 is a nonzero complex-valued constant. In many cases a second (nontrivial) solution $F_2(z)$ exists with the corresponding property

$$F_2(z+d) = \rho_2 F_2(z). \tag{12}$$

The constants $\rho_{1,2}$ are called Floquet (translational) multipliers, and they satisfy the relation

$$\rho_1 = \frac{1}{\rho_2} = e^{i\xi d}, \tag{13}$$

where ξ is called the Bloch wavenumber. The Floquet-Bloch waves can also be written as

$$F_1(z) = P_1(z)e^{i\xi z} \quad \text{and} \quad F_2(z) = P_2(z)e^{-i\xi z}, \tag{14}$$

where both $P_1(z)$ and $P_2(z)$ are smooth periodic functions of period d. Once the solutions $F_1(z)$ and $F_2(z)$ are known on one period (such as on the interval $0 < z < d$), they can be calculated over other periods through recursive application of Eqs. (11) and (12).

The Floquet-Bloch waves can be constructed as

$$v(d) \neq 0: \quad F_{1,2}(z) = u(z) + \frac{\rho_{1,2} - u(d)}{v(d)}v(z), \tag{15}$$

$$u'(d) \neq 0: \quad F_{1,2}(z) = \frac{\rho_{1,2} - v'(d)}{u'(d)}u(z) + v(z), \tag{16}$$

$$v(d) = u'(d) = 0: \quad F_1(z) = u(z),\ F_2(z) = v(z), \tag{17}$$

where $u(z)$ and $v(z)$ are smooth, normalized solutions of Eq. (1), i.e. $u(0) = 1$, $u'(0) = 0$, $v(0) = 0$ and $v'(0) = 1$. The forms of $F_1(z)$ and $F_2(z)$ are determined by the band structure of the periodic potential $Q(z)$. The dispersion relation we use to analyze the band structure is

$$\cos(\xi d) = \frac{u(d) + v'(d)}{2}. \tag{18}$$

Using Eqs. (13) and (18) we can rewrite the Floquet multipliers in the form

$$\rho_{1,2} = \cos(\xi d) \pm i\sqrt{1 - \cos^2(\xi d)}. \tag{19}$$

Regions where $|\cos(\xi d)| < 1$ are called allowed bands. In these regions both Floquet-Bloch waves are bounded, oscillating, complex-valued nonperiodic functions. In addition, the solutions are complex conjugates of one another

$$\begin{aligned} |F_{1,2}(z+d)| &= |F_{1,2}(z)|, \\ \mathrm{Re}[F_1(z)] &= \mathrm{Re}[F_2(z)], \\ \mathrm{Im}[F_1(z)] &= -\mathrm{Im}[F_2(z)]. \end{aligned} \tag{20}$$

Regions where $|\cos(\xi d)| > 1$ are called bandgaps. In these regions both Floquet-Bloch waves are real-valued; one of them decays along the axis of propagation while the other one is unbounded (and thus represents an unphysical solution in an infinite periodic structure)

$$\begin{aligned} |F_1(z+d)| &< |F_1(z)|, \\ |F_2(z+d)| &> |F_2(z)|. \end{aligned} \tag{21}$$

Between the allowed bands and bandgaps, there lie boundaries called bandedges where $|\cos(\xi d)| = 1$. As a result, the Floquet multipliers become identical, $\rho_1 = \rho_2 \equiv \rho = \pm 1$, and the Floquet-Bloch waves become identical periodic functions $F_1(z) = F_2(z) \equiv F(z)$. If $\rho = 1$, the period of $F(z)$ is d and if $\rho = -1$, the period of $F(z)$ is $2d$. If so, another solution to the Hill equation is needed to complete the Floquet-Bloch system, and the most common choice is a function called the hybrid Floquet mode, taking the form

$$G(z) = e^{i\xi z}\left[zP_1(z) + P_2(z)\right], \tag{22}$$

which is a solution of Eq. (1) with the property

$$G(z+d) = \rho G(z) + \rho d F(z). \tag{23}$$

In terms of the smooth normalized solutions, the hybrid Floquet mode is constructed as

$$v(d) \neq 0: \quad G(z) = \frac{\rho d}{v(d)}v(z), \quad \text{or}$$
$$u'(d) \neq 0: \quad G(z) = \frac{\rho d}{u'(d)}u(z). \tag{24}$$

Finally, there are vanishing gaps, also called incipient bands. A vanishing gap is a special kind of bandgap, one that, first, satisfies $|\cos(\xi d)| = 1$ and, second, contains an allowed band in the neighbourhood of each of its points. For example, on a band structure diagram of two independent parameters, a vanishing gap can appear as a point or line [15]. Once again, $\rho_1 = \rho_2 \equiv \rho = \pm 1$, but in addition, unlike on bandedges, $\rho = u(d) = v'(d)$, and the Floquet-Bloch waves $F_1(z)$ and $F_2(z)$ are linearly independent, periodic functions, given by Eq. (17). Thus, in terms of the values of smooth normalized solutions $u(z)$ and $v(z)$ at the point $z = d$, the vanishing gaps are determined by the conditions

$$u(d) = v'(d) = \pm 1, \quad v(d) = u'(d) = 0. \tag{25}$$

Similar to a bandedge, if $\rho = 1$, the period of both Floquet-Bloch waves is d and if $\rho = -1$, their periods are $2d$. Then, any superposition of the Floquet-Bloch waves becomes periodic as well, i.e. in the vanishing gaps any solution of the Hill equation is a periodic function.

4. NEW EXAMPLE A

To begin, we choose the particular solution to Eq. (2) to be

$$\psi_{0\mathrm{A}}(z) = \frac{1}{\sqrt{1 + q\cos^2(z)}}, \qquad q > -1. \tag{26}$$

The constant q must be bounded from below by -1 to avoid singularities in the potential. As mentioned in the previous section, the choice of Eq. (26) is motivated by the desire to find a relatively simple form for Eq. (7). Following the algorithm of Wu and Shih, we construct a periodic potential

$$Q_{\mathrm{A}}(z, a, q) = 1 + a\left[1 + q\cos^2(z)\right]^2 - \frac{2(2+q)}{1 + q\cos^2(z)} + \frac{3(1+q)}{\left[1 + q\cos^2(z)\right]^2}, \tag{27}$$

and its normalized solutions

$$u_{\mathrm{A}}(z) = \sqrt{\frac{1+q}{1 + q\cos^2(z)}}\cos[\Phi_A(z)], \tag{28}$$

$$v_{\mathrm{A}}(z) = \frac{1}{\sqrt{a(1+q)}}\frac{1}{\sqrt{1 + q\cos^2(z)}}\sin\left[\Phi_A(z)\right], \tag{29}$$

where

$$\Phi_{\mathrm{A}}(z) = \sqrt{a}\left[\left[1 + \frac{q}{2}\right]z + \frac{q}{4}\sin(2z)\right]. \tag{30}$$

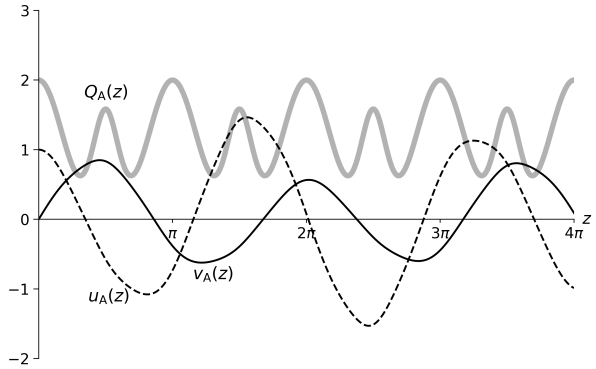

Fig. 1. The normalized solutions $u_{\mathrm{A}}(z)$ (dashed black line) and $v_{\mathrm{A}}(z)$ (solid black line) to the Hill equation with potential $Q_{\mathrm{A}}(z)$ (thick gray line), for $a = 1/2$ and $q = 3/2$. These solutions are continuously differentiable without requiring modification.

The potential and its normalized solutions are illustrated in Fig. (1). It has been constructed with a period of π. To stretch the periods, we need only make the substitution $z \to (\pi/d)z$, which allows us to perform all derivations in this section using the modified potential $Q_{\mathrm{Ad}} = (\pi^2/d^2)Q_{\mathrm{A}}$ of period d. It can easily be checked that Eqs. (28) and (29) satisfy the normalization requirements $u_{\mathrm{A}}(0) = 1$, $u'_{\mathrm{A}}(0) = 0$, $v_{\mathrm{A}}(0) = 0$, and $v'_{\mathrm{A}}(0) = 1$. The potential $Q_{\mathrm{A}}(z)$ is biperiodic with alternating strong and weak oscillations. The relative amplitudes of these oscillations can be modified by varying parameter a. Biperiodic potentials are a subject of interest in various optical systems [16, 17].

A. Determining Band Structure

To analyze the band structure of this potential we refer to the dispersion relation Eq. (18). As with the Casperson and Wu-Shih potentials, we find that $\cos(\xi d) = u_{\mathrm{A}}(d) = v'_{\mathrm{A}}(d)$, leading to

$$\cos(\xi d) = \cos\left[\frac{\pi\sqrt{a}}{2}(q+2)\right]. \tag{31}$$

Eq. (31) indicates that the band structure consists of one bandgap for $a < 0$, one allowed band for $a > 0$, and one bandedge at $a = 0$ separating them.

We then identify incipient bands of this potential by finding all pairs of parameters (a, q) that satisfy Eq. (25). This leads to

$$a = \frac{4m^2}{(q+2)^2}, \qquad m = 1, 2, 3, \ldots. \tag{32}$$

We also find a degenerate incipient band where $q = 0$ and $a > 0$. As was the case with the Takayama, Casperson and Wu-Shih potentials, all incipient bands are composed of continuous lines [9, 10].

The overall band structure is illustrated in Fig. (2). **We should note that the band structure of a typical photonic crystal is plotted as normalized wavenumber (frequency) of propagating light versus one of the parameters of the crystal. Here, the band structure is plotted as a versus q, implying that a plays a role somewhat similar to the normalized frequency of light propagating in a photonic crystal.**

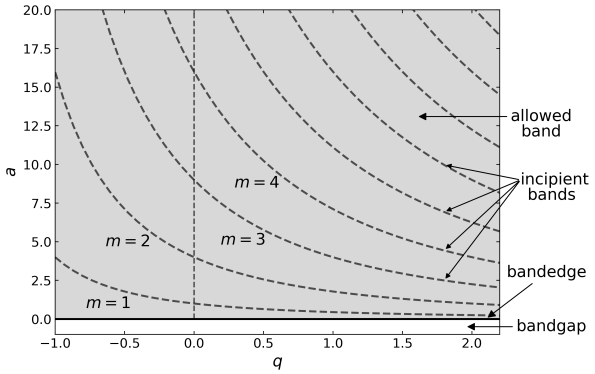

Fig. 2. The band structure for the potential Q_{A}. The bandedge at $a = 0$ (dark horizontal line) separates the bandgap (white background) and the allowed band (gray background). The incipient bands (dashed dark gray lines) are determined by Eq. (32). In addition, there is a degenerate incipient band for $q = 0$, $a > 0$. The first four incipient bands are labeled.

B. Floquet-Bloch System for Allowed Bands and Bandgaps

The Floquet-Bloch fundamental system in the allowed bands and bandgaps consists of two linearly independent Floquet-Bloch waves. To find them for potential A, we begin by using Eq. (19) to obtain the Floquet multipliers

$$\rho_{1,2\mathrm{A}} = \exp\left[\pm i\frac{\pi\sqrt{a}}{2}(q+2)\right]. \tag{33}$$

Together with Eqs. (28) and (29), we can compose the Floquet-Bloch waves, using Eq. (15), as

$$F_{1,2\mathrm{A}}(z) = \sqrt{\frac{1+q}{1+q\cos^2(z)}}\,\exp[\pm i\,\Phi_{\mathrm{A}}(z)]. \tag{34}$$

Note that the Floquet-Bloch solutions are bounded, complex-valued, continuously differentiable, and nonperiodic in the allowed bands. The form of Eq. (34) also makes it clear that they are complex conjugates of one another and obey Eq. (20). However, $\Phi_{\mathrm{A}}(z)$ is imaginary in the bandgap, which turns the oscillations in Eq. (34) into an exponential decay for $F_{1\mathrm{A}}(z)$ and an exponential growth for $F_{2\mathrm{A}}(z)$. Examples of solutions in the allowed band and bandgap are featured in Figs. (3) and (4), respectively.

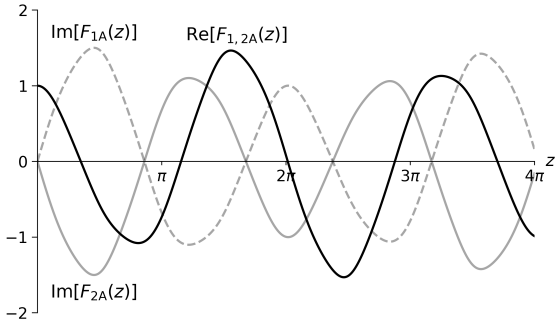

Fig. 3. The real and imaginary components of the Floquet-Bloch waves $F_{1\mathrm{A}}(z)$ and $F_{2\mathrm{A}}(z)$ in the allowed band, for $a = 1/2$ and $q = 3/2$. The real components $\mathrm{Re}[F_{1\mathrm{A}}(z)]$ and $\mathrm{Re}[F_{2\mathrm{A}}(z)]$ (solid black line) coincide, while the imaginary components $\mathrm{Im}[F_{1\mathrm{A}}(z)]$ (dashed gray line) and $\mathrm{Im}[F_{2\mathrm{A}}(z)]$ (solid gray line) are mirror images of each other.

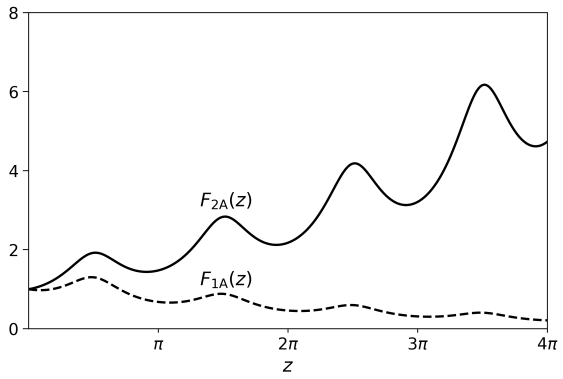

Fig. 4. The Floquet-Bloch solutions $F_{1\mathrm{A}}(z)$ and $F_{2\mathrm{A}}(z)$ in the bandgap, for $a = -1/200$ and $q = 3/2$. The solution $F_{1\mathrm{A}}(z)$ decays, while $F_{2\mathrm{A}}(z)$ rapidly grows.

C. Floquet-Bloch System for Bandedges

At the bandedge we find that $\Phi_{\mathrm{A}}(z) = 0$ for all z, leaving only the solution $F_{1\mathrm{A}}(z) = F_{2\mathrm{A}}(z) \equiv F_{\mathrm{A}}(z)$ available. The Hill equation is a second-order differential equation, so a second solution is needed to complete the Floquet-Bloch fundamental system. We turn to the hybrid Floquet mode, given by Eq. (24).

The first solution, the periodic Floquet-Bloch wave $F_{\mathrm{A}}(z)$, is simply found by setting $a = 0$ in Eq. (34). In this case, $F_{\mathrm{A}}(z)$ coincides with $u_{\mathrm{A}}(z)$, i.e.

$$F_{\mathrm{A}}(z) = \sqrt{\frac{1+q}{1+q\cos^2(z)}}. \tag{35}$$

To find the second solution $G_{\mathrm{A}}(z)$, we first take the limit $a \to 0$ in Eq. (29) and obtain

$$v_{\mathrm{A}}(z) = \frac{(1+q/2)z + (q/4)\sin(2z)}{\sqrt{(1+q)[1+q\cos^2(z)]}}. \tag{36}$$

This form of $v_{\mathrm{A}}(z)$ is suitable for use with Eq. (24), which gives us the hybrid Floquet mode

$$G_{\mathrm{A}}(z) = \left[z + \frac{q}{2(2+q)}\sin(2z)\right]F_{\mathrm{A}}(z). \tag{37}$$

An example of the Floquet-Bloch solutions at the bandedge is shown in Fig. (5).

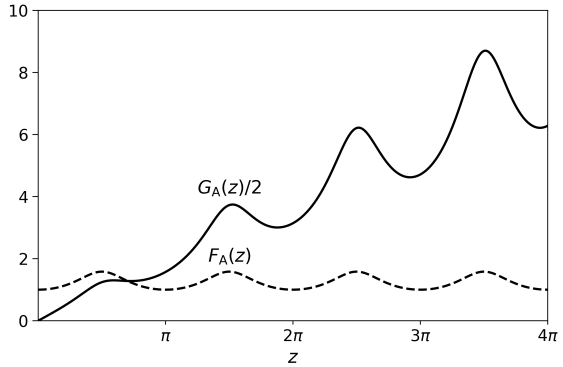

Fig. 5. The Floquet-Bloch wave $F_{\mathrm{A}}(z)$ and hybrid Floquet mode $G_{\mathrm{A}}(z)$ at the bandedge, for $a = 0$ and $q = 3/2$. The solution $F_{\mathrm{A}}(z)$ oscillates periodically while $G_{\mathrm{A}}(z)$ grows without bound.

D. Floquet-Bloch System for Incipient Bands

Incipient bands for this potential are determined by the condition (32). The corresponding incipient periodic Floquet-Bloch waves coincide with the normalized solutions $u_{\rm A}(z)$ and $v_{\rm A}(z)$, given by Eqs. (28) - (30), where we implement the condition (32). This leads to

$$F_{1\rm A}(z) = \sqrt{\frac{1+q}{1+q\cos^2(z)}}\cos[\Phi_{\rm A}(z)]\,, \tag{38}$$

$$F_{2\rm A}(z) = \frac{2+q}{2m\sqrt{1+q}}\frac{1}{\sqrt{1+q\cos^2(z)}}\sin[\Phi_{\rm A}(z)]\,, \tag{39}$$

with

$$\Phi_{\rm A}(z) = m\left[z + \frac{q}{2(2+q)}\sin(2z)\right]. \tag{40}$$

Even and odd values of m correspond to incipient Floquet-Bloch waves with periods of d and $2d$, respectively. Examples for $m = 2$ and $m = 3$ are shown in Figs. (6) and (7).

Finally, in the degenerate incipient band ($q = 0$, $a > 0$), the Floquet-Bloch waves reduce to

$$F_{1\rm A}(z) = \cos(\sqrt{a}z), \tag{41}$$

$$F_{2\rm A}(z) = \frac{1}{\sqrt{a}}\sin(\sqrt{a}z). \tag{42}$$

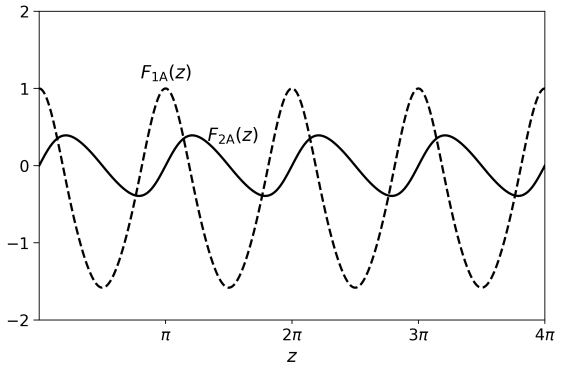

Fig. 6. The Floquet-Bloch waves $F_{1\rm A}(z)$ (dashed black line) and $F_{2\rm A}(z)$ (solid black line) in the incipient band determined by $q = 3/2$ and $m = 2$. Both oscillate with period $d = \pi$, as expected for even values of m.

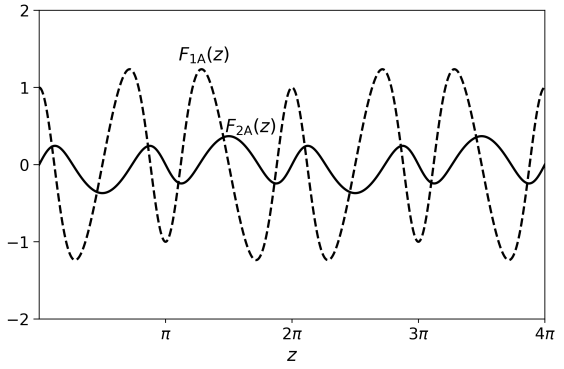

Fig. 7. The Floquet-Bloch waves $F_{1\rm A}(z)$ (dashed black line) and $F_{2\rm A}(z)$ (solid black line) in the incipient band determined by $q = 3/2$ and $m = 3$. Both oscillate with period $2d = 2\pi$, as expected for odd values of m.

5. NEW EXAMPLE B

As the second example we consider the particular solution

$$\psi_{0\rm B}(z) = \frac{1}{\sqrt{1+q[\cos(z)+k\cos(2z)]}}, \tag{43}$$

where $k > -1/3$ is a constant. Define $C_{\rm qk} = 1 + q(1+k)$. To avoid singularities in the potential, q and k must satisfy the restriction $0 < C_{\rm qk} < 2$. Using Eq. (9) we construct the potential

$$\begin{aligned} Q_{\rm B}(z,a,q,k) = a\,[1+q[\cos(z)+k\cos(2z)]]^2 - \\ \frac{1}{2}\frac{q[\cos(z)+4k\cos(2z)]}{[1+q[\cos(z)+k\cos(2z)]]} - \\ \frac{3}{4}\frac{q^2[\sin(z)+2k\sin(2z)]^2}{[1+q[\cos(z)+k\cos(2z)]]^2}\,. \end{aligned} \tag{44}$$

The corresponding normalized solutions are

$$u_{\rm B}(z) = \sqrt{\frac{C_{\rm qk}}{1+q[\cos(z)+k\cos(2z)]}}\cos[\Phi_{\rm B}(z)]\,, \tag{45}$$

$$v_{\rm B}(z) = \frac{1}{\sqrt{a\,C_{\rm qk}}}\frac{1}{\sqrt{1+q[\cos(z)+k\cos(2z)]}}\sin[\Phi_{\rm B}(z)]\,, \tag{46}$$

where the phase integral $\Phi_{\rm B}(z)$ is given by

$$\Phi_{\rm B}(z) = \sqrt{a}\left[z + q\left[\sin(z) + \frac{k}{2}\sin(2z)\right]\right]. \tag{47}$$

This potential and the solutions to its corresponding Hill equation are shown in Fig. (8). As was the case in the first example, we can apply all derivations in this section to a modified potential $Q_{\rm Bd} = (4\pi^2/d^2)Q_{\rm B}$ of period d if we perform the substitution $z \to (2\pi/d)z$.

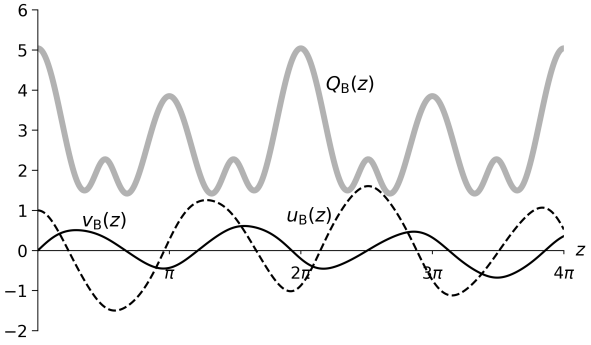

Fig. 8. The triperiodic potential $Q_{\rm B}(z)$ (thick gray line) and the normalized solutions $u_{\rm B}(z)$ (dashed black line) and $v_{\rm B}(z)$ (solid black line) to the corresponding Hill equation, for $a = 5/2$, $k = 5$, and $q = 1/12$.

For large a ($a > 2$), the second and third terms of Eq. (44) are responsible for the low-amplitude oscillations peaking at half-integer multiples of π in Fig. (8). One of the properties of this potential is that we can adjust a to control the contributions of the low-lying oscillations, and then further adjust k to control the relative amplitudes of the higher-amplitude peaks at integer multiples of π.

A. Band Structure

Using the dispersion relation (18), with $u(z)$ and $v(z)$ given by Eqs. (45) and (46), we find

$$\cos(\xi d) = \cos(2\pi\sqrt{a}). \tag{48}$$

The resulting band structure is shown in Fig. (9). As in the first example, this band structure has a single allowed band for $a > 0$, a single bandgap for $a < 0$, and a bandedge between them at $a = 0$. However, the incipient bands are horizontal lines whose position is given by

$$a = \frac{m^2}{4}, \qquad m = 1, 2, 3, \ldots. \tag{49}$$

There is also a degenerate incipient band where $q = 0$ and $a > 0$.

Overall, the band structure is similar in appearance to that of the Takayama potential [10] and is shown in Fig. (9).

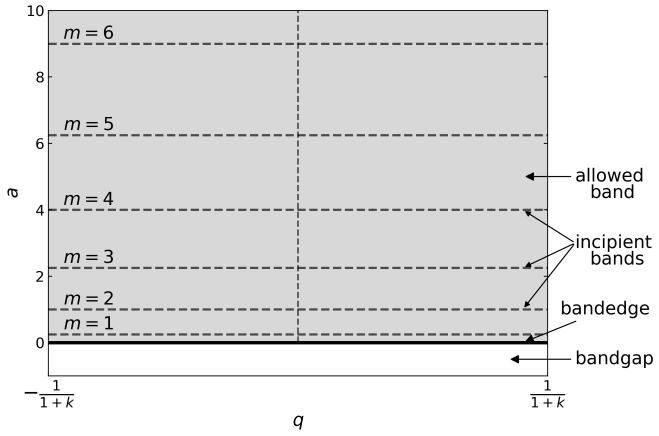

Fig. 9. The band structure for the potential Q_B. The bandedge at $a = 0$ (dark horizontal line) separates the bandgap (white background) and the allowed band (gray background). The horizontal incipient bands (dashed dark gray lines) are determined by Eq. (49). The first six incipient bands are shown.

B. Floquet-Bloch System for Allowed Bands and Bandgaps

Once again we use Eq. (15) to construct the Floquet-Bloch waves in the allowed bands and bandgaps,

$$F_{1,2B}(z) = \sqrt{\frac{C_{qk}}{1 + q[\cos(z) + k\cos(2z)]}}\, \exp[\pm i\, \Phi_B(z)]. \tag{50}$$

As was the case for example A, we see that in the bandgap Eq. (48) becomes purely imaginary, turning the complex oscillations in Eq. (50) into a real exponential decay/growth. Examples of the Floquet-Bloch solutions in the allowed band and bandgap are provided in Figs. (10) and (11), respectively.

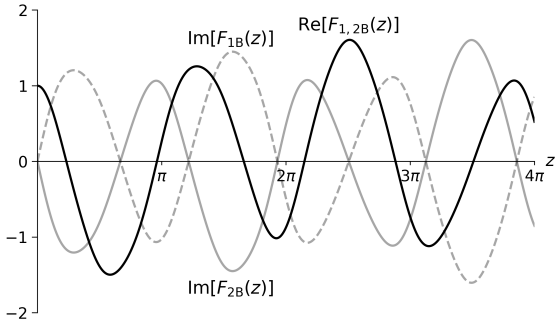

Fig. 10. The Floquet-Bloch waves $F_{1B}(z)$ and $F_{2B}(z)$ in the allowed band, for $a = 5/2$, $k = 5$, and $q = 1/12$. The real components $\mathrm{Re}[F_{1B}(z)]$ and $\mathrm{Re}[F_{2B}(z)]$ (solid black line) coincide, while the imaginary components $\mathrm{Im}[F_{1B}(z)]$ (dashed gray line) and $\mathrm{Im}[F_{2B}(z)]$ (solid gray line) are opposite in sign.

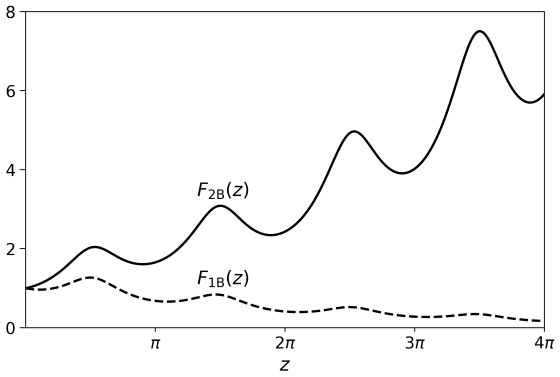

Fig. 11. The Floquet-Bloch solutions $F_{1B}(z)$ and $F_{2B}(z)$ in the bandgap, for $a = -1/50$, $k = 5$ and $q = 1/12$. The solution $F_{1B}(z)$ decays, while $F_{2B}(z)$ rapidly grows.

C. Floquet-Bloch System for Bandedges

The bandedge $a = 0$ gives us a single Floquet-Bloch wave $F_{1B}(z) = F_{2B}(z) \equiv F_B(z)$, and we again turn to Eq. (24) to create the hybrid Floquet mode $G_B(z)$. This leads to the Floquet-Bloch solutions of the form

$$F_B(z) = \sqrt{\frac{C_{qk}}{1 + q[\cos(z) + k\cos(2z)]}}, \tag{51}$$

$$G_B(z) = \left[z + q\left[\sin(z) + \frac{k}{2}\sin(2z)\right]\right] F_B(z). \tag{52}$$

Examples of those solutions are shown in Fig. (12). The Floquet-Bloch solutions for potentials $Q_A(z)$ and $Q_B(z)$ at the bandedge are very similar in appearance; one can compare Figs. (5) and (12).

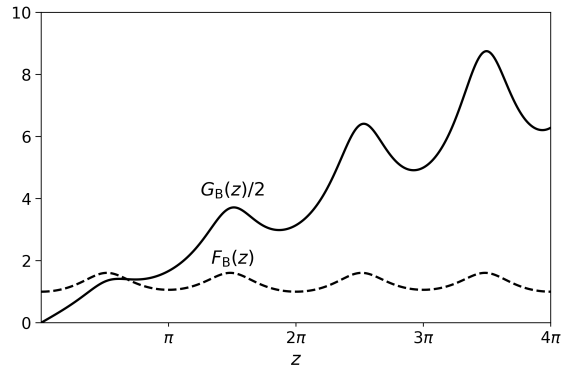

Fig. 12. The Floquet-Bloch wave $F_B(z)$ and hybrid Floquet mode $G_B(z)$ in the bandedge, for $a = 0$, $k = 5$, and $q = 1/12$. The solution $F_B(z)$ oscillates periodically while $G_B(z)$ grows without bound.

D. Floquet-Bloch System for Incipient Bands

Picking locations on the band structure that satisfy Eq. (49) allows us to identify the incipient bands. As in example A, the incipient periodic Floquet-Bloch waves coincide with the solutions $u_B(z)$ and $v_B(z)$, and can be rewritten as

$$F_{1B}(z) = \sqrt{\frac{C_{qk}}{1+q[\cos(z)+k\cos(2z)]}}\cos[\Phi_B(z)]\,, \tag{53}$$

$$F_{2B}(z) = \frac{2}{m\sqrt{C_{qk}}}\frac{1}{\sqrt{1+q[\cos(z)+k\cos(2z)]}}\sin[\Phi_B(z)]\,, \tag{54}$$

where

$$\Phi_B(z) = \frac{m}{2}\left[z+q\left[\sin(z)+\frac{1}{2}k\sin(2z)\right]\right]. \tag{55}$$

In Fig. (13) we see an example of incipient Floquet-Bloch waves when m is odd and $\rho = -1$; both waves have a period of $2d = 4\pi$. Likewise, in Fig. (14) is shown an example of incipient Floquet-Bloch waves when m is even and $\rho = 1$; both waves have a period $d = 2\pi$.

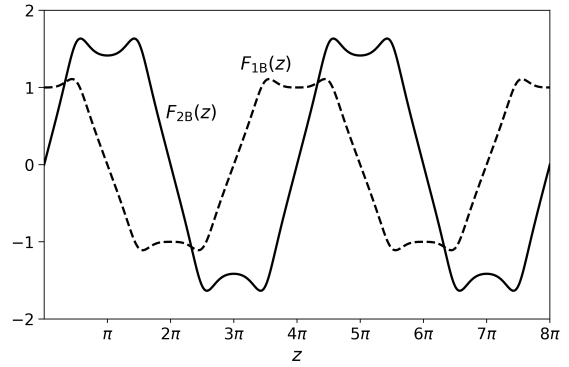

Fig. 13. The Floquet-Bloch waves $F_{1B}(z)$ (dashed black line) and $F_{2B}(z)$ (solid black line) in the incipient band determined by $k = 5$, $q = 1/12$ and $m = 1$. Both oscillate with period $2d = 4\pi$, as expected for odd values of m.

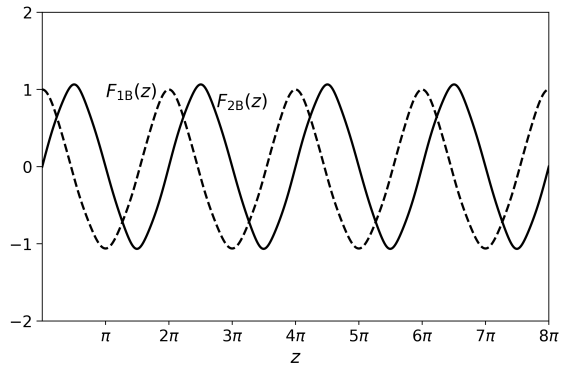

Fig. 14. The Floquet-Bloch waves $F_{1B}(z)$ (dashed black line) and $F_{2B}(z)$ (solid black line) in the incipient band determined by $k = 5$, $q = 1/12$ and $m = 2$. Both oscillate with period $d = 2\pi$, as expected for even values of m.

6. NEW EXAMPLE C

Our third example begins with the particular solution

$$\psi_{0C}(z) = \sqrt{\frac{1+q\sin(z)}{1+q\cos(z)}}, \tag{56}$$

where $-1 < q < 1$ is a constant. **This example is somewhat different from the previous two. As we mentioned in section 2, we try to pick a solution ψ_0 in the form given by Eq. (8), where, in particular, $g(z)$ is a nonvanishing function. As one can see that is the case with the first two examples, but not with the current one. As a result, the phase integrals given by Eq. (7) might have jump discontinuities and further adjustments might be needed to construct smooth normalized solutions of the corresponding potential. However, the framework remains the same.** Using Eq. (4) we construct the potential

$$Q_C(z,a,q) = \frac{a[1+q\cos(z)]^2+(1/4)q^2\cos^2(z)}{[1+q\sin(z)]^2} - \frac{3}{4}\frac{q^2\sin^2(z)}{[1+q\cos(z)]^2} - \frac{1}{2}\left[\frac{q^2\sin(z)\cos(z)+q\cos(z)-q\sin(z)}{[1+q\cos(z)][1+q\sin(z)]}\right]. \tag{57}$$

Its normalized solutions are

$$u_C(z) = \sqrt{1+q+\frac{1}{4a}\frac{q^2}{(1+q)}}\sqrt{\frac{1+q\sin(z)}{1+q\cos(z)}}\cos[\Phi_{1C}(z)], \tag{58}$$

$$v_C(z) = \frac{1}{\sqrt{a(1+q)}}\sqrt{\frac{1+q\sin(z)}{1+q\cos(z)}}\sin[\Phi_{2C}(z)]. \tag{59}$$

Their respective phase integrals are given by

$$\Phi_{1,2C}(z) = \sqrt{a}\left[\frac{2}{\sqrt{1-q^2}}\arctan\left[\frac{q+\tan(z/2)}{\sqrt{1-q^2}}\right] + \ln[1+q\sin(z)]\right] + D_{1,2}, \tag{60}$$

where

$$D_1 = D_2 + \arctan\left[\frac{1}{2\sqrt{a}}\frac{q}{(1+q)}\right], \tag{61}$$

$$D_2 = -2\sqrt{\frac{a}{1-q^2}}\arctan\left[\frac{q}{\sqrt{1-q^2}}\right]. \tag{62}$$

The above solutions $u_C(z)$ and $v_C(z)$ have jump discontinuities at points $z_j = d/2 + jd$, $j = 1, 2, 3, ...$, where $d = 2\pi$ is the period of potential $Q_C(z)$. We construct smooth versions of those solutions by redefining the phase integrals (60) as

$$\Phi_{1,2C}(z) = \sqrt{a}\left[\frac{2}{\sqrt{1-q^2}}\left[(j-1)\pi + \arctan\left[\frac{q+\tan(z/2)}{\sqrt{1-q^2}}\right]\right] + \ln[1+q\sin(z)]\right] + D_{1,2}\,, \tag{63}$$

where $j = 1$ for $-\pi < z < \pi$, $j = 2$ for $\pi < z < 3\pi$, etc.

The potential $Q_C(z)$ and its smooth normalized solutions are shown in Fig. (15). Unlike potentials A and B, $Q_C(z)$ is more sawtooth-like in appearance. For large values of a ($a > 3$), the low-amplitude oscillations peaking at odd integer multiples of π can be made negligible.

As in the examples A and B, derivations in this section apply to a modified potential $Q_{Cd} = (4\pi^2/d^2)Q_C$ of period d after performing the substitution $z \to (2\pi/d)z$.

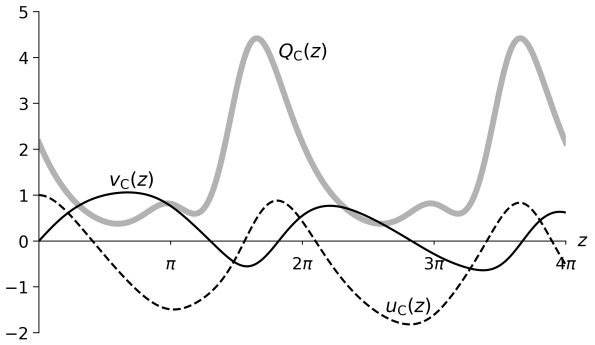

Fig. 15. The normalized solutions $u_C(z)$ (dashed black line) and $v_C(z)$ (solid black line) to the Hill equation with potential $Q_C(z)$ (thick gray line), for $a = 1$ and $q = 3/2$.

A. Band Structure

We again use the dispersion relation (18), with $u(z)$ and $v(z)$ given this time by Eqs. (58) and (59), to find

$$\cos(\xi d) = \cos\left[2\pi\sqrt{\frac{a}{1-q^2}}\right]. \tag{64}$$

The locations of the bandgap, allowed band, and bandedge are identical to those of the first two examples. The incipient bands come in the form of lines given by

$$a = \frac{m^2}{4}(1-q^2), \qquad m = 1, 2, 3, \ldots. \tag{65}$$

The degenerate incipient band is found where $q = 0$ and $a > 0$. The resulting band structure, shown in Fig. (16), is identical to that of the Wu-Shih potential, save for a multiplicative factor of $1/4$ for the incipient bands [9].

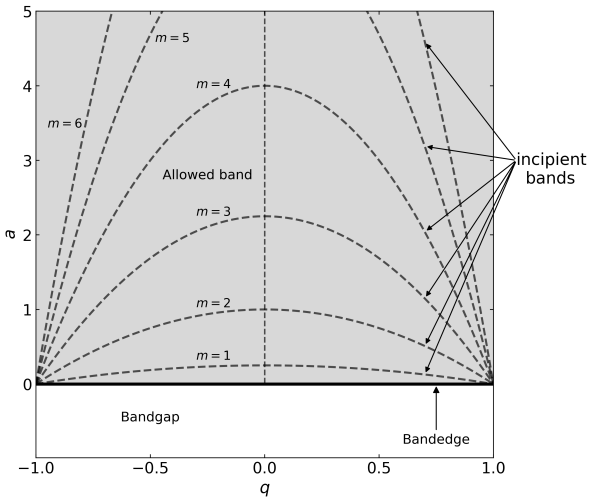

Fig. 16. The band structure for the potential Q_C. The bandedge at $a = 0$ (dark horizontal line) separates the bandgap (white background) and the allowed band (gray background). The incipient bands (dashed dark gray lines) are determined by Eq. (65). The first six incipient bands are illustrated.

B. Floquet-Bloch System for Allowed Bands and Bandgaps

Using Eq. (15) to construct the Floquet-Bloch waves in the allowed bands and bandgaps, we find

$$F_{1,2C} = \sqrt{1+q}\sqrt{\frac{1+q\sin(z)}{1+q\cos(z)}}\exp[\pm i\Phi_C(z)]. \tag{66}$$

In the allowed band Eq. (66) takes the form of complex oscillations, while in the bandgap it turns into a real exponential decay/growth. The Floquet-Bloch solutions in the allowed band and bandgap are provided in Figs. (17) and (18) respectively, displaying very similar properties to their counterparts of examples A and B.

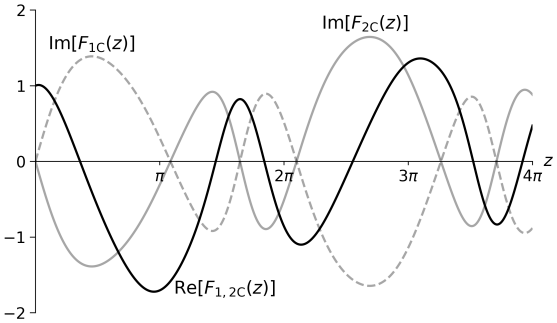

Fig. 17. The Floquet-Bloch waves $F_{1C}(z)$ and $F_{2C}(z)$ in the allowed band, for $a = 3/2$ and $q = 1/2$. The real components $\mathrm{Re}[F_{1C}(z)]$ and $\mathrm{Re}[F_{2C}(z)]$ (solid black line) coincide, while the imaginary components $\mathrm{Im}[F_{1C}(z)]$ (dashed gray line) and $\mathrm{Im}[F_{2C}(z)]$ (solid gray line) are opposite in sign.

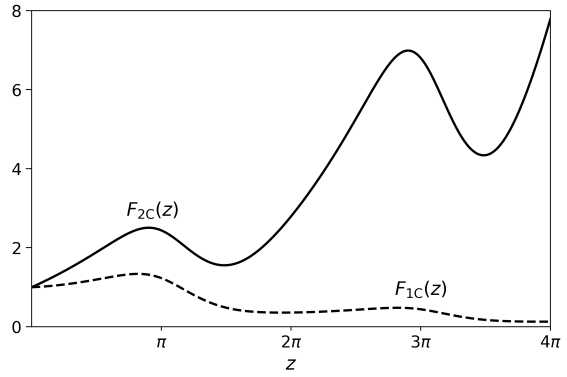

Fig. 18. The Floquet-Bloch solutions $F_{1C}(z)$ and $F_{2C}(z)$ in the bandgap, for $a = -1/50$ and $q = 1/2$. The solution $F_{1C}(z)$ decays, while $F_{2C}(z)$ rapidly grows.

C. Floquet-Bloch System for Bandedges

At the bandedge we once again have for the Floquet-Bloch waves

$$F_{1C}(z) = F_{2C}(z) \equiv F_C(z) = \sqrt{1+q}\sqrt{\frac{1+q\sin(z)}{1+q\cos(z)}}. \quad (67)$$

Then, we use Eq. (24) to construct the hybrid Floquet mode $G_C(z)$ in the form

$$G_C(z) = \left\{2(j-1)\pi + 2\arctan\left[\frac{q+\tan(z/2)}{\sqrt{1-q^2}}\right] - 2\arctan\left[\frac{q}{\sqrt{1-q^2}}\right] + \sqrt{1-q^2}\ln\left[1+q\sin(z)\right]\right\} F_C(z). \quad (68)$$

The above bandedge Floquet-Bloch solutions (67) and (68) are shown in Fig. (19).

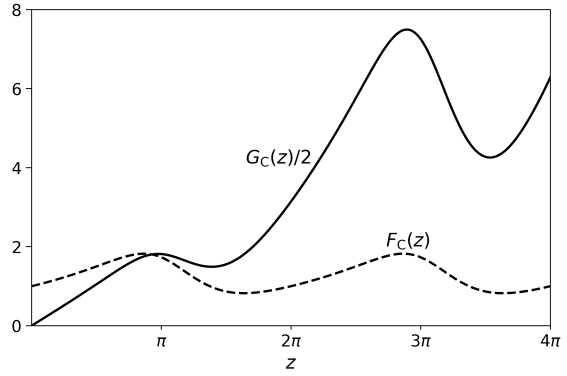

Fig. 19. The Floquet-Bloch wave $F_C(z)$ and hybrid Floquet mode $G_C(z)$ at the bandedge, for $a = 0$ and $q = 1/2$. The solution $F_C(z)$ oscillates periodically, while $G_C(z)$ grows without bound.

D. Floquet-Bloch System for Incipient Bands

As was the case for potentials A and B, the Floquet-Bloch waves in the incipient bands coincide with the smooth solutions $u_C(z)$ and $v_C(z)$. They are constructed by choosing pairs of parameters a and q that satisfy Eq. (65).

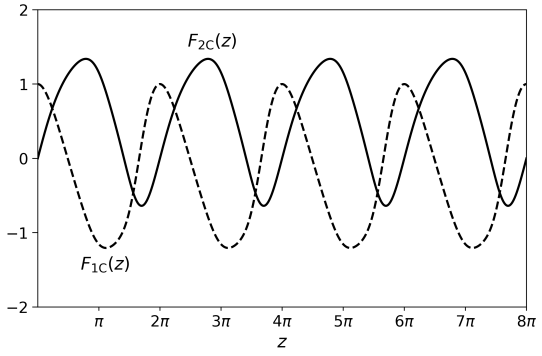

Fig. 20. The Floquet-Bloch waves $F_{1C}(z)$ (dashed black line) and $F_{2C}(z)$ (solid black line) in the incipient band determined by $q = 1/2$ and $m = 2$. Both oscillate with period $d = 2\pi$, as expected for even values of m.

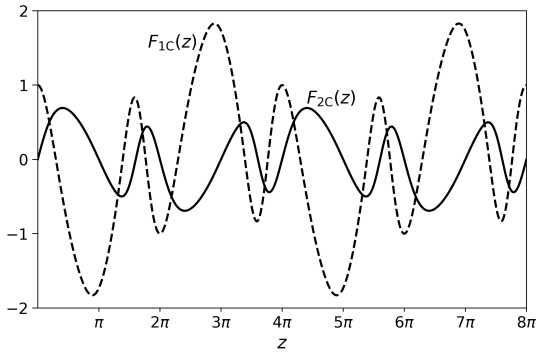

Fig. 21. The Floquet-Bloch waves $F_{1C}(z)$ (dashed black line) and $F_{2C}(z)$ (solid black line) in the incipient band determined by $q = 1/2$ and $m = 3$. Both oscillate with period $2d = 4\pi$, as expected for odd values of m.

Figures 20 and 21 show the incipient periodic Floquet-Bloch waves when $m = 2$ and $m = 3$, respectively.

7. SUMMARY

We used the Wu-Shih procedure to construct three analytically solvable Hill equations with smooth potentials and solutions. We found the band structure of each potential using the dispersion relation for the Bloch wavenumber. All three band structures share similarities with those of the Takayama, Casperson, and Wu-Shih potentials. They all have a single allowed band and a single bandgap, separated by a bandedge boundary, as well as a set of incipient bands in the form of continuous lines dividing their respective allowed bands. We then constructed Floquet-Bloch solutions in every characteristic region (allowed band, band gap, bandedge, incipient band) of the band structure of each potential. The use of the Wu-Shih procedure along with Floquet-Bloch theory has the possibility of being useful for constructing potentials that model optical structures **with continuous refractive index, in particular, rugate filters**.

8. FUNDING INFORMATION

DWLS is grateful to NSERC Canada for support under Discovery Grant RGPIN-3198.

REFERENCES

1. G. Allen, "Band structures of one-dimensional crystals with square-well potentials," Phys. Rev. **91**, 531–533 (1953).
2. G. V. Morozov, D. W. L. Sprung, and J. Martorell, "One-dimensional photonic crystals with a sawtooth refractive index: another exactly solvable potential," New J. Phys. **15**, 103009 (2013).
3. A. A. Cottey, "Floquet's theorem and band theory in one dimension," Am. J. Phys. **39**, 1235–1244 (1971).
4. S. Caffrey, G. V. Morozov, D. W. L. Sprung, and J. Martorell, "Floquet-Bloch solutions in a sawtooth photonic crystal," Opt. Quantum Electron. **49**, 112 (2017).
5. L. W. Casperson, "Solvable Hill equation," Phys. Rev. A **30**, 2749–2751 (1984).
6. L. W. Casperson, "Erratum: Solvable Hill equation," Phys. Rev. A **31**, 2743–2743 (1985).
7. K. Takayama, "Note on solvable Hill equations," Phys. Rev. A **34**, 4408–4410 (1986).
8. S. M. Wu and C. C. Shih, "Construction of solvable Hill equations," Phys. Rev. A **32**, 3736–3738 (1985).
9. S. Caffrey, G. V. Morozov, D. MacBeath, and D. W. L. Sprung, "Floquet-Bloch analysis of analytically solvable Hill equations with continuous potentials," J. Opt. Soc. Am. B **33**, 1190–1196 (2016).
10. G. V. Morozov and D. W. L. Sprung, "Band structure analysis of an analytically solvable Hill equation with continuous potential," J. Opt. **17**, 035607 (2015).
11. B. G. Bovard, "Rugate filter theory: an overview," App. Opt. **32**, 5427–5442 (1993).
12. M. J. Renne, "Comment on "solvable Hill equation"," Phys. Rev. A **33**, 4430–4430 (1986).
13. G. V. Morozov and D. W. L. Sprung, "Floquet-Bloch waves in one-dimensional photonic crystals," EPL (Europhys. Lett.) **96**, 54005 (2011).
14. G. V. Morozov and D. W. L. Sprung, "Transverse-magnetic-polarized Floquet-Bloch waves in one-dimensional photonic crystals," J. Opt. Soc. Am. B **29**, 3231–3239 (2012).
15. S. Caffrey, G. V. Morozov, D. Macbeath, and D. W. L. Sprung, "Vanishing gaps in photonic crystals and other periodic potentials," (*Proceedings of 18th International Conference on Transparent Optical Networks (ICTON)*, 2016).
16. D. W. L. Sprung, L. W. A. Vanderspek, W. van Dijk, J. Martorell, and C. Pacher, "Biperiodic superlattices and the transparent state," Phys. Rev. B **77**, 035333 (2008).
17. S. Rist, P. Vignolo, and G. Morigi, "Photonic spectrum of bichromatic optical lattices," Phys. Rev. A **79**, 053822 (2009).